Journal of Research in Pharmacy

Research Article

www.jrespharm.com

Deciphering the antimicrobial and cytotoxic impact of *Aspergillus terreus*-biogenic silver nanoparticles

Nourhan KHALAF [1], Nageh ABO-DAHAB [1], Bahig EL-DEEB [2], Abdallah HASSANE [1,*]

[1] Department of Botany and Microbiology, Faculty of Science, Al-Azhar University, Assiut Branch, Assiut 71524, Egypt.
[2] Department of Botany and Microbiology, Faculty of Science, Sohag University, Sohag 82524, Egypt.
* Corresponding Author. E-mail: abdallahhassane@azhar.edu.eg (A.H.); Tel. +20-1122990125.

Received: 5 December 2024 / Revised: 6 January 2025 / Accepted: 11 January 2025

ABSTRACT: Nanobiotechnology is a grow-fast applied scientific discipline and has established straight forward shots in medicine, agriculture, and industry. Herein, an investigation on the myco-synthesis of silver nanoparticles (AgNPs) extracellularly by, soil molecularly identified strain, *Aspergillus terreus* was carried out. Bio-fabricated AgNPs were characterized and inspected for their antibacterial, antifungal, and cytotoxic potency. UV–Visible wave analysis of AgNPs revealed a surface plasmon resonance band at 427 nm. The TEM analysis exhibited spherical particles diameter size ranged between 11 and 30 nm, while AgNPs' crystalline nature was confirmed by XRD. Zeta potential value was found to be -16.4 with well dispersed and spherical particles with average size of 27.4 nm. At a concentration of 5000 µg/mL, AgNPs showed antimicrobial efficiency against subjected pathogenic bacterial and *Candida* species with MICs values ranging from 15.62 to 104.16 µg/mL for antibacterial potency and 125 to 104.16 µg/mL for anticandidal efficacy. Biogenic AgNPs cytotoxicity assay afforded cells viability of 17.8% against HepG2 cell line at 10 µg/mL, meanwhile *Artemia salina* LC_{50} mortality was established at 95.32 µg/mL. These findings suggest that biosynthesized AgNPs have promising potent cytotoxicity and antimicrobial issue for treating pathogenic infections.

KEYWORDS: *Aspergillus terreus*; biosynthesis; silver nanoparticles; antibacterial; anticandidal; cytotoxicity.

1. INTRODUCTION

Bio-nanotechnology refers to synthesis of nanoparticles using biological systems [1]. Nanotechnology has been employed broadly in several applications comprising medicine, agriculture, electronics, photonics, catalysis, chemo-sensing and imaging, environmental remediation, biolabeling, and drug delivery, due to its particular characteristics such as size, shape, chemical compositions, and elevated ratio of surface area to volume [2]. Despite the developments in chemical and physical synthetic approaches of metallic nanoparticles [3,4], biological methods remain the preferred eco-friendly and cost-efficient synthesis approach [5].

Among biological systems, fungi including soil, endophytic, epiphytic, and mycorrhizal isolates are heterotrophs where their primary and secondary metabolites conferring their economic importance. They offered a variety of biological activities and biotechnological applications. This encompasses nutraceutical, medical, and biotechnological polysaccharides, lipids and fatty acids, and enzymes and peptides as well as low molecular weight secondary products exhibiting different antibacterial, antifungal, anticancer, antioxidant, wound healing, and/or even toxigenic (mycotoxins) properties [6-13].

Metal nanoparticles (MtNPs) are made of the metals precursors and has unique opt-electrical properties because of their surface plasma resonance characteristic [14]. Potential bio-factories for the environmentally friendly synthesis of MtNPs are thought to be microorganisms, thus due to the diversity of species enabled to react with metal ions during the production of MtNPs [15] generating MtNPs with a defined shape, size, composition, and monodispersed particles [16]. Enzymes and/or secondary metabolites that are released by fungal cells are used as reducing agents when metallic ions are reduced to create myco-nanoparticles [17]. Regarding extracellular synthesis of MtNPs, fungi produce elevated protein ratios, which significantly modify the fabrication of nanoparticles [18]. Fungi gained varied advantages over other microbial systems for biogenesis of NPs comprising easier to develop media, scale-up, downstream, increased proteins generation, and simple biomass preparation [19]. In addition, fungal enzymes increase the number of synthesized nanoparticles, act as stabilizing agents, and preventing MtNPs agglomeration [20].

How to cite this article: Khalaf N, Abo-Dahab N, El-Deeb B, Hassane A. Deciphering the antimicrobial and cytotoxic impact of Aspergillus terreus-biogenic silver nanoparticles. J Res Pharm. 2025; 29(4): 1760-1774.

ISSN: 2630-6344

https://dx.doi.org/10.12991/jrespharm.1734921

Recently, there has been a lot of interest in silver nanoparticles (AgNPs) due to their safety for applications in biomedicine and biotechnology [21]. Silver NPs established several bioactivities such as antimicrobial, wound healing, anti-viral, anti-inflammatory, of phytopathogens control, anti-cancer, antioxidants, DNA delivery, and biosensors [22]. These activities could be attributed to catalytic activity, bio-compatibility, stability, high conductivity, and extensive surface area of AgNPs [23]. Numerous fungal species have been utilized to produce AgNPs extracellularly including *Aspergillus terreus* Thom, *A. niger* Tiegh, *Penicillium aurantiogriseum* Dierckx, *Metacordyceps chlamydosporia* Evans (formerly *Verticillium chlamydosporium*), *Trichoderma gamsii* Samuels & Druzhin, and *Rhizopus arrhizus* [24,25]. In this regard, the present investigation aimed to affirm, up-to-date, the potent bioactivity of AgNPs-mediated mycosynthesis. Thus, further *in vivo* and pharmaceutical studies may be conducted to approve their incorporation in applicable pharmaceutics.

2. RESULTS

This study dealt with biosynthesis of AgNPs using *Aspergillus terreus* extracellular filtrate, followed by AgNPs characterization utilizing UV-Vis, XRD, TEM, FTIR, and DLS analysis. Biosynthesized AgNPs antimicrobial potency were assessed against a variety of fungal and bacterial pathogens, in addition to an *in vitro* cytotoxicity evaluation against HepG2 cell line.

2.1. Phylogenetic analysis of fungal isolate

Identification was performed through sequencing of ITS loci and sequences were undergone to BLAST within NCBI database. The isolate was identified as *A. terreus* AUMC15440 (GenBank accession no. OR840515). *Aspergillus terreus* AUMC15440, aligned with closely relevant strains from the GenBank, exhibited 99.83% - 100% identity and 99% - 100% coverage with multiple strains of the same species encompassing the type strain *A. terreus* ATCC1012 (NR_137472) (Figures 1 and 2).

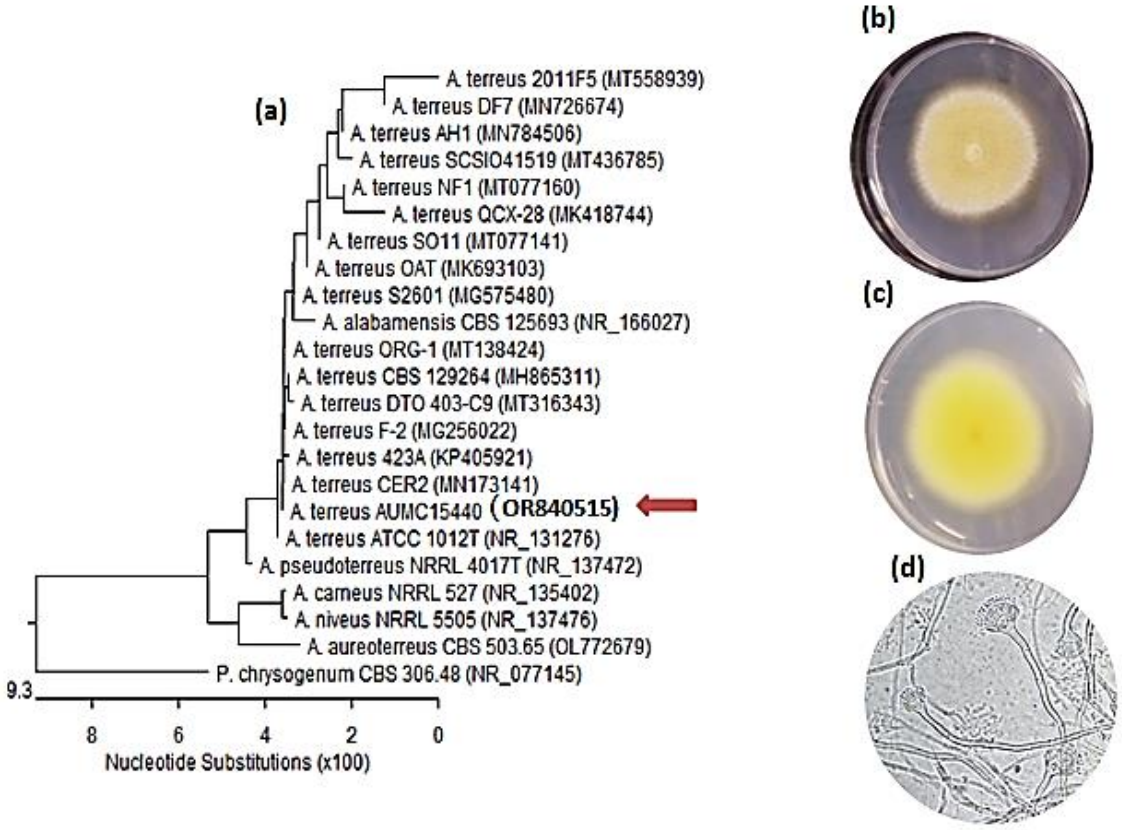

Figure 1. *Aspergillus terreus* AUMC15440; (a) Phylogenetic tree depended on the ITS sequences, and (b-d) cultural characteristics; microscopic magnification 400x.

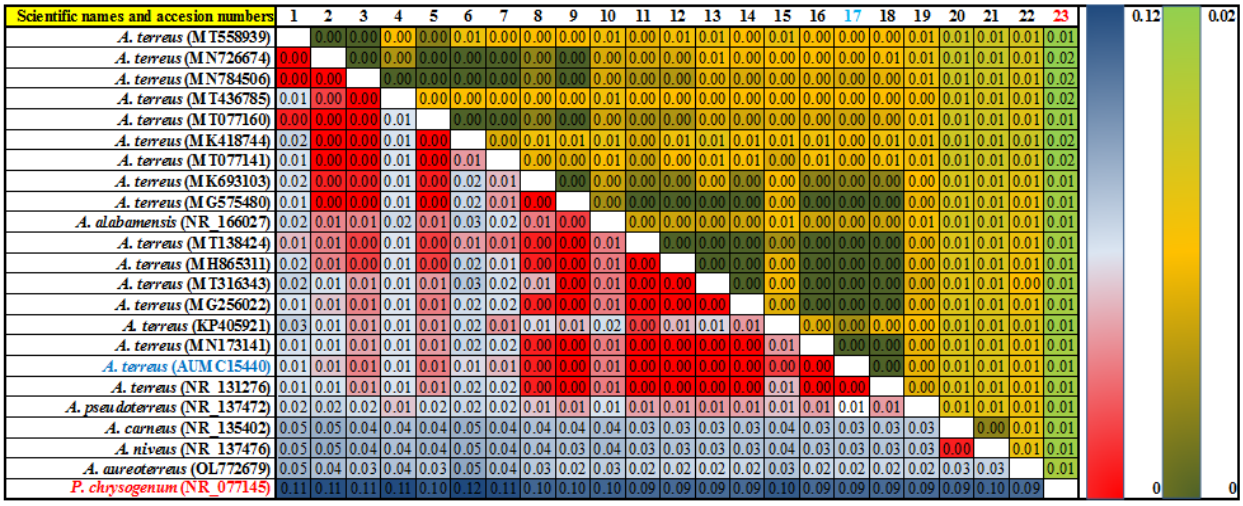

Figure 2. A heat map analysis of *A. terreus* AUMC15440 (OR840515) phylogenetic tree.

2.2. Characterization of biosynthesized nanoparticles

The color of fungal filtrate turned into brown color after treatment with $AgNO_3$ and incubation in dark for one day (Figure 3A). UV–Visible wave analysis of AgNPs manifested SPR band at 427 nm (Figure 3B). Silver nanoparticles crystalline characteristic was established using XRD analysis which revealed the metal silver's ideal structure of face centered cubic (fcc). The XRD spectra, at 2θ values, exhibited five pioneer Bragg diffraction peaks of 38.1°, 44.2°, 64.4°, 77.4°, and 81.539° that were compatible with 111, 200, 202, 311, and 222 fcc AgNPs planes, respectively. The diffraction peaks were consonant with standard database files (JCPDS card No. 9008459), which confirmed that the myco-synthesized AgNPs possessed a crystalline nature (Figure 4). Transmission electron microscopy showed spherical AgNPs with size ranging from 11 to 30 nm in diameter (Figure 5).

The DLS measurements revealed the fabrication of spherical well-dispersed AgNPs with 27.4 nm average size distribution (Figure 6). A negative zeta potential of -16.4±0.32 mV was observed (Figure 7). The high zeta potential absolute value declared the involvement of highly electrical charge on AgNPs surface. So, strong repulsive force may be constituted among the particles spaces which prevented agglomeration and indicated a very stable AgNPs in the colloidal state.

The spectral FTIR analysis of myco-synthesized AgNPs exposed a number of diversified bands comprising strong bands appeared at 2946.97 and 2910.07cm^{-1} which indicated aliphatic C–H stretching, while C–H stretching of aldehyde at 2830.59 and 2669.55 cm^{-1} was indicated. At 1615.48 cm^{-1}, the appeared band indicated N-H related to amine, while carbonyl group (C=O) stretching band was represented at 1512.45cm^{-1}. Moreover, bands centered at 1007.31 and 1339.06 cm^{-1} were owed to S=O and C-O functional stretchings, respectively (Figure 8).

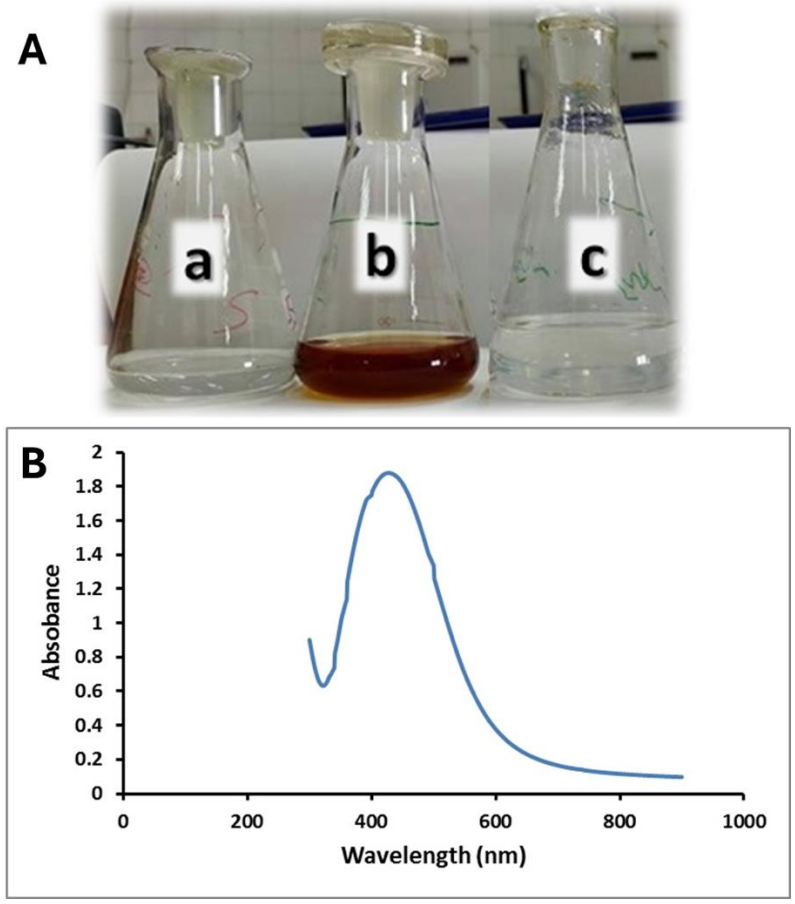

Figure 3. (A) Flasks containing **a)** AgNO3, **b)** fungal filtrate combined silver nitrate (AgNPs), and **c)** fungal filtrate without silver nitrate. **(B)** UV–Vis absorption band of AgNPs.

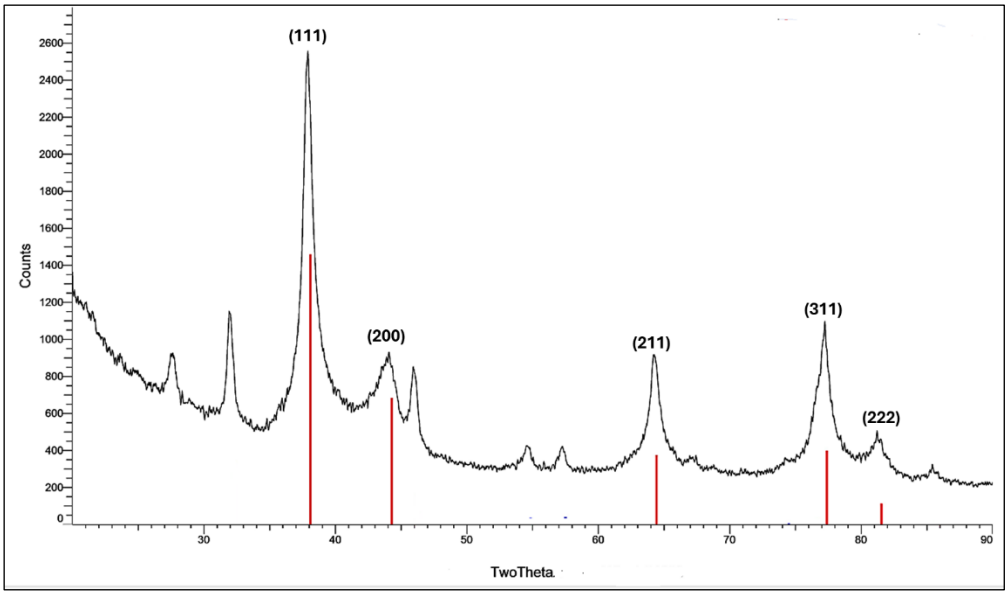

Figure 4. XRD micrograph of biofabricated AgNPs.

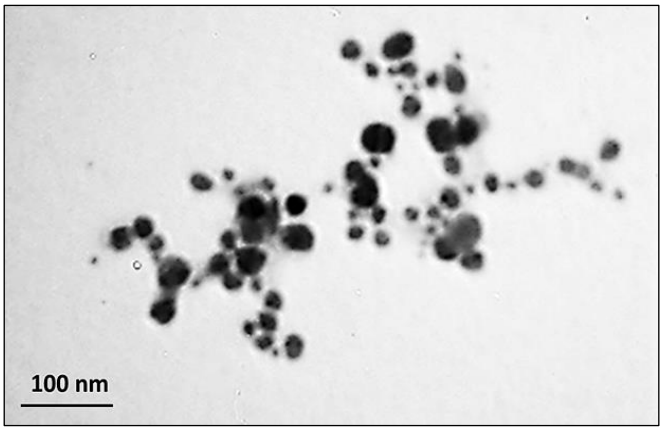

Figure 5. TEM image of biogenic AgNPs.

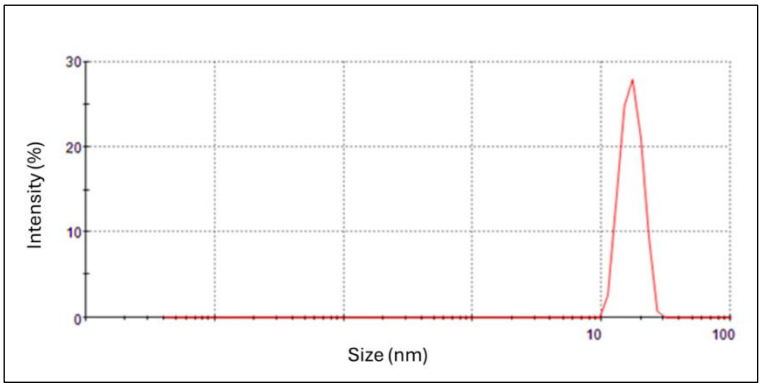

Figure 6. Dynamic light scattering measurements for particle size distribution of the mycosynthesized AgNPs.

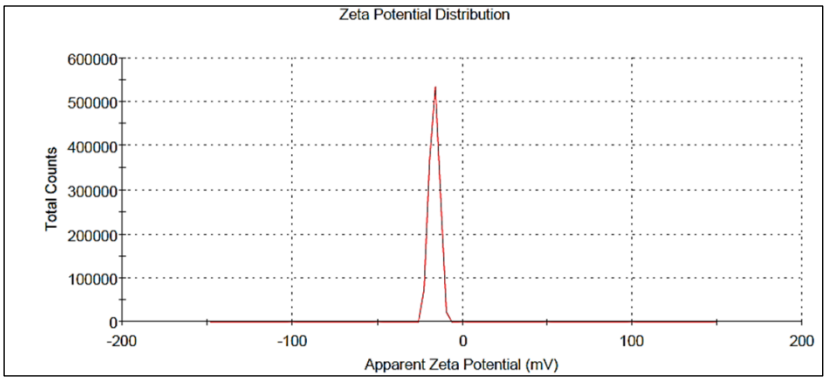

Figure 7. Zeta potential measurements of the mycosynthesized AgNPs.

2.3. Antimicrobial activity and MICs of AgNPs

Different concentrations of AgNPs (5000 to 10 µg/mL) exhibited antibacterial activity at all tested concentrations against *B. subtilis, S. aureus, E. coli, K. pneumonia, S. typhi,* and *S. marcescens* with zone of inhibition ranged from 29.60 to 9.80 mm diameter, while *P. vulgaris* and *P. aeruginosa* showed resistance to AgNPs at concentrations 20 and 300 µg/mL, respectively. Silver nanoparticles at 5000 µg/mL exhibited inhibition of bacterial growth with diameters of 29.60, 28.80, 27.00, 25.50, 24.50, 24.00, 21.60, and 20.80 mm against *B. subtilis, S. aureus, S. typhi*, *S. marcescens, E. coli, P. vulgaris*, *K. pneumonia,* and *P. aeruginosa,* respectively, (Figure 9) and MICs values of 10, 10, 10, 10, 40, 400, and 10 µg/mL, respectively. Chloramphenicol showed antibacterial activity against whole bacterial species with diameters of inhibition zones ranged from 38.00 to 14.00 mm. Using INT assay, silver nanoparticles reported MICs of 104.16, 52.08, 31.25, 31.25, 20.83, 20.83, 15.62, and 15.62 µg/mL against *P. vulgaris*, *P. aeruginosa*, *S. aureus*, *E. coli*, *S. typhi*, *K. pneumonia*, *B. subtilis*, and *S. marcescens,* respectively (Figure 10).

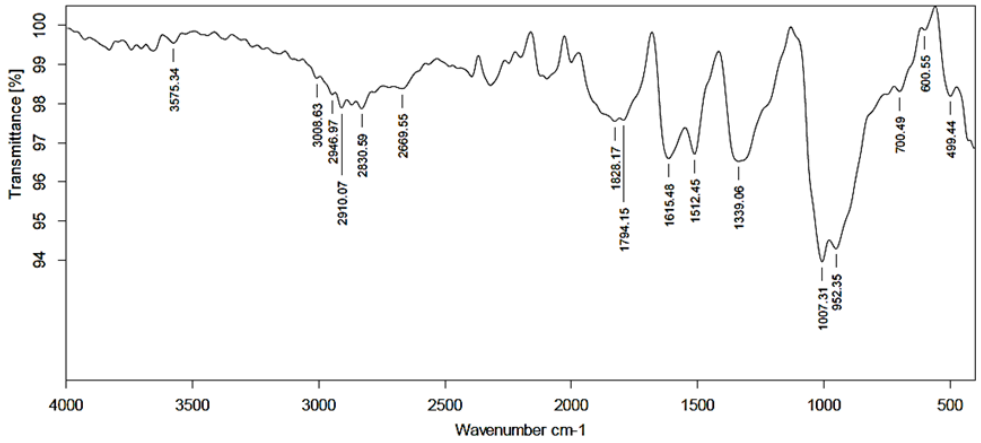

Figure 8. FTIR analysis of biosynthesized AgNPs.

Antifungal activity of AgNPs at 5000 µg/mL inhibited the growth of *C. albicans*, *C. krusei*, and *C. glabrata* strains with inhibition zone diameters 10.50, 11.60, and 13.30 mm, respectively. Other test concentrations of AgNPs did not affect the *Candida* spp. On the other hand, AgNPs had no effect on the growth of *G. candidum* and *R. mucilaginosa* (Figure 11). Utilizing broth dilution assay, silver nanoparticles reported MICs of 208.33, 125, and 125 µg/mL against *C. glabrata, C.krusei,* and *C. albican*, respectively (Figure 12). Clotrimazole inhibited of the growth of all fungal species with inhibition zone diameters ranged from 20.60 to 27.00 mm.

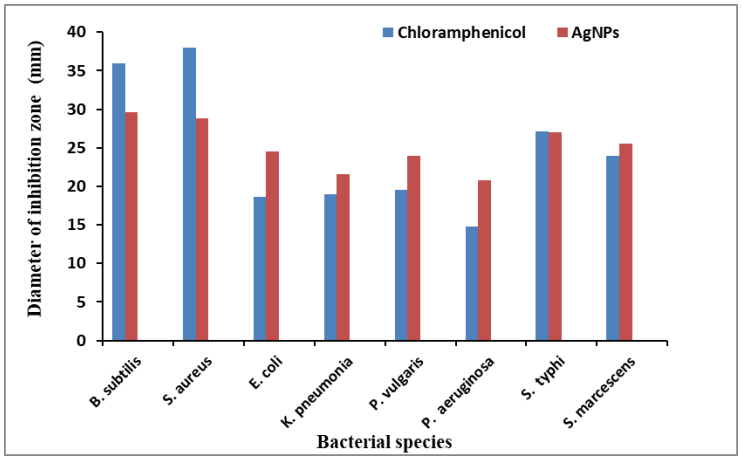

Figure 9. Antibacterial activity of AgNPs (5000 µg/mL) and chloramphenicol (1 mg/mL).

2.4. Cytotoxicity assay of AgNPs

The lethality of *Artemia salina* larvae was discovered to be directly proportional to AgNPs concentration. Maximum mortality rate was observed at 200 µg/mL concentration while LC_{50} mortality was indicated at 95.32 µg/mL concentration. *In vitro* antitumor potency of the AgNPs was assessed against HepG2 cell line at two concentrations (100 and 10 µg/mL). *In vitro* AgNPs cytotoxicity assay against HepG2 cell line at concentration 100 µg/mL exhibited 4.83% viability, while at 10 µg/mL, cells' viability was 17.80%. Standard doxorubicin in comparison with AgNPs showed high viability of HepG2 cell at tested concentration (Table 1).

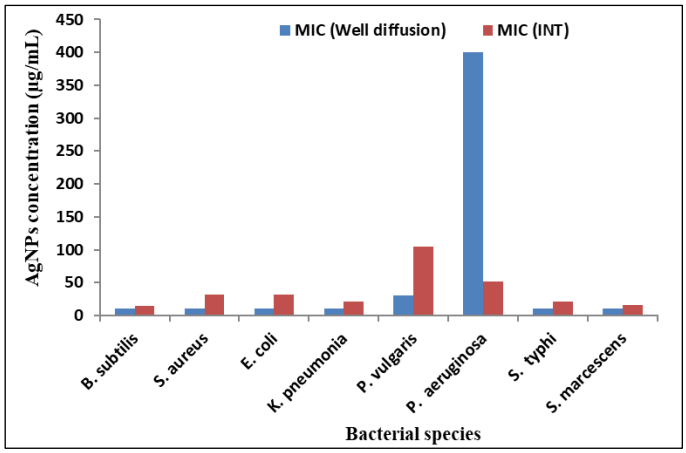

Figure 10. Antibacterial MICs value AgNPs by well diffusion and INT methods.

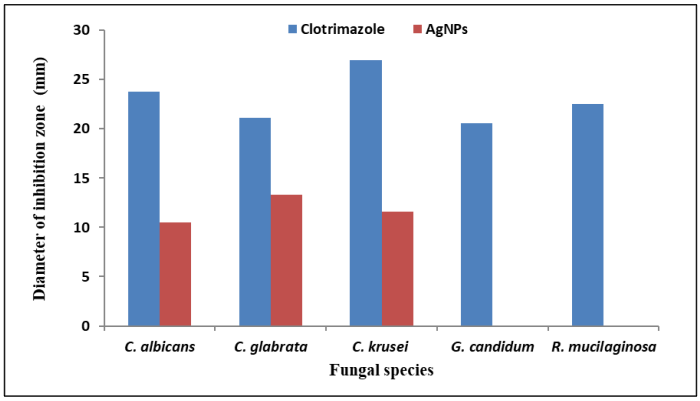

Figure 11. Antifungal activity of AgNPs (5000 µg/mL) and clotrimazole (1 mg/mL) against tested fungal strains.

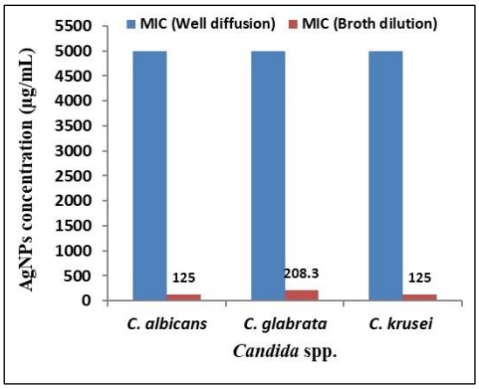

Figure 12. Anticandidal MICs values AgNPs using well diffusion and broth dilution assays.

Table 1. Cytotoxicity impact of AgNPs against HepG2 cell line and *Artemia salina*.

Tested compound	HepG2 viability %		*Artemia salina* LC_{50} (µg/mL)
	100 µg/mL	10 µg/mL	
AgNPs	4.83	17.80	95.32
Dox	23.80	88.87	

2.5. Mechanistic modes of AgNPs antimicrobial and cytotoxic efficacy

Nano-sized AgNPs possessed many principal modes of antimicrobial action, in both Gram-positive and Gram-negative bacteria, fungi, and animal cells including adhesion to bacterial cell wall and phospholipid membranes leading to their disrupter, penetration into the cell and damage of membrane-bounded organelles, ribosomes, enzymes, DNA causing their destabilization, induction of oxidative stress via generating reactive oxygen species (ROS) leading to cell death (apoptosis), and modulation of cellular signaling affecting growth of bacteria, division, and other cellular reactions (Figure 13).

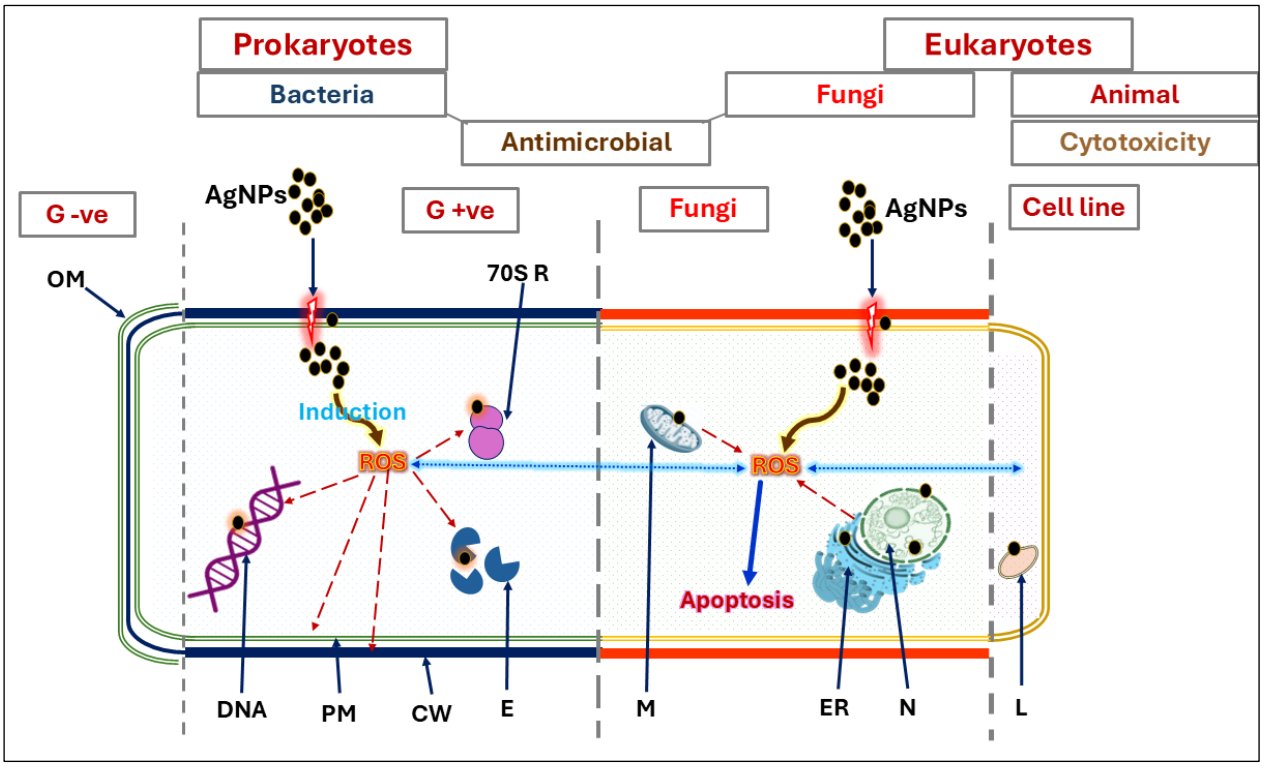

Figure 13. The antimicrobial and cytotoxic mechanisms scheme of nanoparticles; OM (outer membrane), PM (plasma membrane), CW (cell wall), E (enzymes), 70S R (70S ribosome), M (mitochondrion), ER (endoplasmic reticulum), N (nucleus), L (lysosome), and ROS (reactive oxygen species).

3. DISCUSSION

The mycosynthesis of silver nanoparticles encompasses advantages including high biomass production, facility of handling and cultivation, and the ability to produce elevated quantities of enzymes end bioactive metabolites. These molecules responsible for synthesis nanoparticles and forming capping agent responsible for stability and activity of nanoparticles [26]. Biosynthesis of silver nanoparticles carried out by biomolecules of microorganism such as those mated with the complex pathways including electron transport during the transformation of NADPH/NADH to $NADP^+$/NAD^+ [27].

In the present study, molecular identification using ITS sequences and phylogenetic characterization of *A. terreus* AUMC15440 was carried out. Both ends of the ITS region disclosed nucleotide sequence variations in the multiple alignment [28]. Lazreg et al. [29] reported that the 5.8S rDNA nucleotide sequences were proved to have ideal homology, while Mohamed *et al.* [30] stated that the ITS loci represent essential effective markers for confirming identification of fungal strains at the species level. Mazrou *et al.* [31] and Al Mousa *et al.* [11] indicated that using the molecular approach, utilizing ITS region sequencing, for identifying *Aspergillus* spp. strains was an efficient tool to validate their identification.

Regarding characterization of myco-synthesized AgNPs by *A. terreus* extracellular reducing agent filtrate, Baymiller *et al.* [32] reported that NAD-dependent nitrate reductase enzyme is essential in biosynthesis of metallic nanoparticles. Our findings were compatible with preceding studies, where UV–Vis analysis revealed SPR band at 427 nm, spherical particles with size in diameter between 11 and 30 nm

by TEM analysis, crystalline nature by XRD. -16.4 zeta potential value, and well dispersed spherical particles with average size of 27.4 nm.

Lotfy *et al.* [33] reported that synthesized AgNPs using *A. terreus* mycelial filtrate, after incubation with $AgNO_3$ for 2 days, changed from yellow to dark brown color. Lotfy *et al.* [33] and Mossa *et al.* [34] revealed that extracellulary mycosynthesized AgNPs utilizing *A. terreus* filtrates gave a peak at 420 nm. Results of TEM examination showed agreement with Lotfy *et al.* [33] who produced spherical and poly-dispersed AgNPs ranging from 7 to 23 nm using endophytic *A. terreus*, while Mossa *et al.* [34] synthesized spherical AgNPs ranging from 3 to 60 nm.

The XRD peaks detected in the present investigation were in agreement with Lotfy *et al.* [33] who confirmed diffraction peaks at 2θ equals 38.06°, 44.39°, 64.4° and 77.29° that are analogous to 111, 200, 220, and 311 lattice plane of biosynthesized AgNPs. These results indicated that the biofabricated AgNPs possessed crystalline nature and nanoscale size [35].

The DLS analysis according to Hashem *et al.* [36] exhibited biosynthesized AgNPs with an average size of 32.7 nm and a size distribution histogram from 30 to 47 nm, while Saied *et al.* [37] reported average diameter sizes of 78 nm for biosynthesized AgNPs using *Rhizopus oryzae*. The data from the zeta potential assay in the current investigation agreed with that obtained by Balakumaran *et al.* [38] who indicated the −ve zeta potential of *A. terreus*-synthesized AgNPs. The NPs negative value suggested to be attributed to the presence of the reducing constituents within fungal filtrate, which affords electrostatic forces in biosynthesized NPs [39] (Nasrollahzadeh and Sajadi, 2016). Divyalakshmi and Thoppil [40] explained that DLS analysis was utilized to affirm the size and particle distribution of NPs in colloidal solutions and because of its sensitivity to the presence of aggregates, it is found to be more appropriate for early-stage aggregation monitoring.

The FTIR spectrum of AgNPs exposed diverse bands involving numerous stretching related to aldehyde, amine, carbonyl group, and functional C-O stretching and S=O stretching groups. These findings are consistent with other observations of synthesized AgNPs by *Aspergillus flavus* GGRK1 [41,42]. The detected bands of functional groups proved their preferable ability to bind with silver ions and coat AgNPs to prevent clustering and settle down the medium [43].

According to our results, AgNPs presented potency against all assayed pathogenic bacterial species and *Candida* spp. with MICs values ranging from 15.62 to 104.16 µg/mL for antibacterial influence and from 104.16 to 125 µg/mL for anticandidal activity. In this context, mycosynthesized AgNPs showed inhibition zones of 19.3, 14.9, and 22.0 mm toward *E.coli, S. aureus* and *B. subtilis* were, respectively [44]. Vijayakumar *et al.* [45] observed high sensitivity of *S. aureus* to be to mycosynthesized AgNPs, with 11 mm zone of inhibition, pursued by *B. subtilis* and *P. aeruginosa* (4 mm) and *E. coli* (3 mm). Moreover, Saied *et al.* [44] reported that *B. subtilis* and *E. coli* were more susceptible to AgNPs with MICs of 62.5 µg/mL, while antifungal influence against *C. albicans* and *A. brasiliensis* was observed at 500 and 1000 µg/mL, respectively.

Mohanta *et al.* [46] suggested that the bactericidal impact of AgNPs could be brought on by the electrostatic interactions existed between charged positively AgNPs and negatively bacterial cells. Furthermore, Priyadarshni *et al.* [47] assumed that AgNPs' physicochemical characteristics have produce some alterations that making them efficient antibacterial drugs due to their higher surface area-to-volume ratio. The NPs antimicrobial specificity is interconnected to their total surface area, hence, the smaller particles in size, the fast invasion of bacterial cells will be occurred [48].

Artemia salina larvae cytotoxicity assay of *A. terreus* biosynthesized AgNPs afforded LC_{50} mortality at 95.32 µg/mL. *Artemia salina* larvae cytotoxicity assay represents rapid and cost-effective test to inspect the toxicity or safety of fungal extracts [49,50]. Cytotoxcicty of AgNPs *in vitro* assay against HepG2 cell line at 100 and 10 µg/mL exhibited 4.83% and 17.80 % cell viability, respectively. Our observation agreed with Mossa *et al.* [34] who reported increased AgNPs cytotoxicity with increased concentration against human normal fibroblast cells (BJ), where at 100 µg/ml, *A. terreus* AgNPs exhibited 32.5% inhibition. These findings suggest that concentrations below 100 µg/mL could be effective against diseased cells while minimizing harm to healthy cells.

Han *et al.* [51] demonstrated the enhanced cytotoxicity of biosynthesized AgNPs compared to their synthetic counterparts where biosynthesized AgNPs had an IC_{50} value of 20 µg/mL against human lung epithelial adenocarcinoma cell lines, whereas synthetic AgNPs required a higher concentration of 70 µg/mL to achieve the same effect. Silver nanoparticles have the potential to disrupt cellular proteins' normal functions and cause ensuing alterations in cellular chemistry [52]. Morones *et al.* [53] suggested that the cytotoxic effects of AgNPs are attributable to interact with thiol-rich enzymes. Gharpure *et al.* [54] showed

the selective toxicity of NPs to bio-parameters including cellular membrane structure and cell physiological conditions, while Andleeb *et al*. [55] indicated that IC_{50} values are depending on NPs sizes, shapes, biocompatibility, and surface reactivity. Cao *et al.* [56] suggest that tight bounding between NPs and phytochemical coating affects their release and penetrating of the cell, which results in reduction of their bio-efficacy.

4. CONCLUSION

Silver nanoparticles, AgNPs, were bio-fabricated *via* a green synthesis using *A. terreus* extracelluar filtrate. Various characterization tools were utilized, including UV-Vis, TEM, XRD, DLS, and FTIR. TEM analysis revealed spherical with average size of 11 to 30 nm AgNPs, while XRD affirmed crystallinity nature. Zeta potential value was found to be -16.4 mV with hydrodynamic particle of 27.4 nm. Biosynthesized AgNPs offered reasonable antimicrobial activity against diverse G+ve and G-ve bacteria and *Candida* spp. High potent anticancer activity against HepG2 cell line was observed. These findings suggest that AgNPs have significant potential for treating infections and could be further optimized for safe, convenient, and biocompatible clinical use. Further study will be conducted to ensure more efficiency of AgNPs regarding stability and bioactivity and to be introduced into other biotechnological applications.

5. MATERIALS AND METHODS

5.1. Isolation and identification of the fungus

Dilution-plate method [57] was used to isolate *Aspergillus terreus*, from cement sample obtained from cement factory at Assiut, Egypt (27°10′48.4824″N, 31°11′21.4188″E), on Czapek's (Cz) agar medium. Isolate was characterized according to macro-morphology and microscopic properties, and maintained at Assiut University Mycological Center culture collection (AUMC).

5.1.1. Identification of the isolated fungus using molecular approach

According to Mazrou *et al.* [31] and Mohamed *et al.* [58], the molecular and phylogenetic analysis of the fungus isolate was attained. For the amplification of the ITS region, universal primers including ITS-1 sequence (5′-TCC GTA GGT GAA CCT GCG G-3′) and ITS-4 sequence (5′-TCC TCC GCT TAT TGA TAT GC-3′) were utilized for the DNA amplification using PCR. All obtained PCR outcomes were sequenced and tested isolate identification was confirmed by comparing with strains sequences acquired from database sequences utilizing GenBank BLAST (http:// www.ncbi.nlm.nih.gov/BLAST/).

5.2. Biosynthesis of AgNPs

Silver nitrate, with molecular weight of 169.87 g/mole, was prepared by dissolving 1.69 g in 50 mL of deionized water to obtain stock solution with 200 mM concentration.

Fungal isolate was inoculated in sterilized Czapek's broth and incubated on orbital shaker (160 rpm) for 5 days at 28±2 °C. After that, the fungal biomass was collected by filtration followed by rinsing using distilled water many times. Ten grams of fungal biomass were immersed in 200 mL of sterilized double distilled water for 48 h at 28±2 °C on 160 rpm agitation. After that, the cell filtrate was obtained by filtration and 100 mL was combined with 100 mL 3 mM silver nitrate to attain a concentration of 1.5 mM. The mixture was kept at room temperature in dark conditions for 24 h [59]. After color change, the AgNPs was centrifuged for 15 minutes at 14,000 rpm. Repeated washing was done to take out impurities and the AgNPs were collected.

5.3. AgNPs Characterization

Characterization of AgNPs was performed following the techniques as reported by Yassin *et al.* [60] and Khalaf *et al.* [61]. The bioconversion of silver nitrate salt solution into AgNPs was observed visually by color alteration that established the reduction process. AgNPs were confirmed using UV-Visible spectrophotometer (UV-Vis; Jasco V-530) with readings between 200 to 700 nm at room temperature for detecting the existence of recognizable of AgNPs surface plasmon resonance (SPR) bands. The forms of the biosynthesized AgNPs were inspected by transmission electron microscope (TEM; JEOL/JEM-2100, HRTEM, Tokyo, Japan). Fourier Transform Infrared Spectroscopy (FTIR; 6100, Perkin-Elmer, Germany) was employed to inspect the prominent functional groups coating the AgNPs surface at a resolution of 4 cm^{-1}

and wavelength ranging from 400–4000 cm^{-1}. X-ray diffractometer (XRD; Panalytical X'PERT PRO) was employed to confirm the presence of elemental AgNPs by scanning the 2ø diffraction of 5–90° range. Photon correlation spectroscopy using particle size analyzer and dynamic light scattering (DLS; Zetasizer Nano ZN, Malvern Panalytical Ltd, United Kingdom) was employed for determining AgNPs particle size (average diameters) and size distribution (polydispersity index) at fixed angle of 173° at 25°.

5.4. Antimicrobial susceptibility assay

5.4.1. Test microorganisms

Gram-positive bacteria (*Bacillus subtilis* ATCC6633 and *Staphylococcus aureus* ATCC6538) and Gram-negative bacteria (*Escherichia coli* ATCC8739, *Klebsiella pneumonia* ATCC43816, *Proteus vulgaris* AUH123, *Pseudomonas aeruginosa* ATCC9027, *Salmonella typhi* AUH71, and *Serratia marcescens* AUH98) in addition to fungal isolates (*Candida albicans* ATCC10231, *C. krusei* TU87, *C. glabrata* TU52, *Geotrichum candidum* TU65 [ON430507], and *Rhodotorula mucilaginosa* [ON459714]) were used as test pathogenic microbes [11,62,63]. The bacterial isolates were cultivated in Mueller-Hinton broth for one day at 37 °C, while fungal isolates were inoculated in Sabouraud dextrose broth for 48 h at 25 °C for 2 days.

5.4.2. Agar well diffusion method

The antimicrobial susceptibility assay was carried out as described by Jahangirian *et al.* [64] using well diffusion technique with 8 mm well diameter hold with 100 µL of well dispersed, by sonication, 5000 µg/mL AgNPs. Clotrimazole and chloramphenicol, at concentration of 1 mg/mL, were used for fungi and bacteria as positive control, respectively. Muller-Hinton and Sabouraud dextrose plates impregnated with broth cultures of the assayed bacterial and fungal species were used for evaluating AgNPs antimicrobial potency. The diameter of inhibition zone surrounding the well (in millimeter) was employed to express positive efficiency. Same procedure was repeated for dilutions of AgNPs at gradual concentrations ranging from 4000 to 10 µg/mL to determine the AgNPs minimum inhibitory concentration (MIC).

5.4.3. Determination of MIC using the p-iodonitrotetrazolium chloride (INT) broth dilution assay

The MICs of AgNPs were assessed using the INT micro dilution colorimetric approach as depicted by Gebreyohannes *et al.* [65]. Preparation of AgNPs was executed by dissolving 8000 µg of nanoparticles in 1 mL double distilled water. Eppendorf tubes filled with 1000 µL of sterile nutrient broth were diluted serially with nanoparticles to attain diverse concentrations ranged from 8000 to 15.625 µg/mL, respectively. A 50 µL inoculum size (1.0×10^5 CFU/mL) was added into the Eppendorf tubes. Positive control included 1000 µL of nutrient broth and 50 µL of bacterial suspension, while negative control contained only the nutrient broth. After that, all Eppendorf tubes were incubated for one day at 37 °C. The MIC for antibacterial activity was estimated by addition of 80 µL (2 mg/mL) of 0.02% INT and incubation for half hour at 37 °C. The INT was utilized to indicate bacterial growth, where bacterial cells metabolize INT and alters it to pink color. Unchanged color of INT represents an indication of no bacterial growth.

5.4.4. Determination of MIC using the broth dilution assay

For determining the MIC for antifungal activity, broth dilution assay was utilized as described for antibacterial assay without the use of INT. In addition, Sabouraud dextrose broth was utilized and the inoculated treated tubes as well as control tubes were incubated at 25 °C for two days.

5.5. Cytotoxicity assay

5.5.1. Brine shrimp cytotoxicity assay

The brine shrimp cytotoxicity test was employed by dispersing AgNPs in ddH_2O at varied concentrations (200–10 µg g/mL), and then a 100 µL of each conc. was compiled in glass tubes containing 4.9 mL of seawater containing living 10 brine shrimp larvae. The number of living larvae was counted in each tube after 24 h. The determination of the lethal concentration of the extract and Se NPs that killed 50% of the larvae (LC_{50}) was estimated using probit analysis [66].

5.5.2. Cell culture cytotoxicity assay

Hepatocellular carcinoma cell line (HepG2) was provided by Nawah Scientific Inc., Cairo, Egypt, preserved at 37 °C in DMEM medium amended with 100 units/mL of penicillin, 100 mg/mL of streptomycin, and 10% of heat-inactivated (FBS) fetal bovine serum in 5% (*v/v*) CO_2 humidified atmosphere. Cell viability was assessed in a 96-well plate as reported by Skehan *et al.* [67] and Alsehli *et al.* [68] using SRB assay followed by incubation for 24 h. After that, cells were handled with 100 µL medium containing green fabricated AgNPs at 100 and 10 µg/mL, respectively, and doxorubicin was used as standard positive control. After treatment, cells were stabilized by 10% TCA and preserved at 4 °C for 1 h, rinsed with deionized water, and then 70 µL of 0.4% SRB solution (w/v) was compiled and kept in dark for 10 min at room temperature. Plates were rinsed with acetic acid (1%), overnight air-dried, and then 150 µL of TRIS (10mM) was mixed to solubilize SRB protein-bound stain.Using Infinite F50 microplate reader (TECAN, Switzerland) at 540 nm, absorbance was measured and IC_{50} value was calculated.

Author contributions: Concept – A.H., N.A.; Design – A.H., N.A., B.E.; Supervision – N.A.; Resources – A.H., N.K.; Materials – N.K.; Data Collection and Processing – A.H., N.K.; Analysis and Interpretation – A.H., N.A., B.E.; Literature Search – A.H., N.K.; Writing – A.H., N.K.; Critical Reviews – A.H., N.A., B.E.

Conflict of interest statement: The authors declared no conflict of interest.

REFERENCES

[1] Abdel-Aziz SM, Prasad R, El Enshasy H. and Sukmawati D. Prospects of microbial nanotechnology for promoting climate resilient agriculture. In : Nanoparticles and Plant-Microbe Interactions. Seena S, Rai R, Kumar S, Eds. Elsevier, 2023; pp.163–186. https://doi.org/10.1016/B978-0-323-90619-7.00006-0

[2] Salem SS, El-Belely EF, Niedbała G, Alnoman MM, Hassan SE-D, Eid AM, Shaheen TI, Elkelish A. and Fouda A. Bactericidal and *in-vitro* cytotoxic efficacy of silver nanoparticles (Ag-NPs) fabricated by endophytic actinomycetes and their use as coating for the textile fabrics. Nanomaterials.2020; 10(10): 2082. https://doi.org/10.3390/nano10102082

[3] Abdel-Rahim RD, Al-Ansari SH, Ali GAM, Hassane AMA, Kamoun EA, Gomaa H. and Nagiub AM. A hybrid nanocomposite of silver nanoparticles embedded with end-of-life battery-derived sheets-like nitrogen and sulfur-doped reduced-graphene oxide for water treatment and antimicrobial applications. Water, Air, and Soil Pollution. 2024; 235: 623. https://doi.org/10.1007/s11270-024-07387-9

[4] Kamal A, Hassane AMA, An C, Deng Q, Hu N, Abolibda TZ, Altaleb HA, Gomha SM, Selim MM, Shenashen MA. and Gomaa H. Developing a cost-efective and eco-friendly adsorbent/photocatalyst using biomass and urban waste for crystal violet removal and antimicrobial applications. Biomass Convers Biorefinery. 2024; 2204: 1-19. https://doi.org/10.1007/s13399-024-05850-5

[5] Salem SS. Bio-fabrication of selenium nanoparticles using baker's yeast extract and its antimicrobial efficacy on food borne pathogens. Appl Biochem Biotechnol. 2022; 194: 1898–1910. https://doi.org/10.1007/s12010-022-03809-8

[6] Abo-Dahab NF, Abdel-Hadi AM, Abdul-Raouf UM, El-Shanawany AA. and Hassane AMA. Qualitative detection of aflatoxins and aflatoxigenic fungi in wheat flour from different regions of Egypt. IOSR J Environ Sci Toxicol Food Technol. 2016; 10(7–II): 20-26. https://doi.org/10.9790/2402-1007022026.

[7] Hassane AMA, Hussien SM, Abouelela ME, Taha, TM, Awad MF, Mohamed H, Hassan MM, Hassan MHA, Abo-Dahab NF. and El-Shanawany A-RA. *In vitro* and *in silico* antioxidant efficiency of bio-potent secondary metabolites from different taxa of black seed-producing plants and their derived mycoendophytes. Front Bioeng Biotechnol. 2022; 10: 930161. https://doi.org/10.3389/fbioe.2022.930161

[8] Mohamed H, Awad MF, Shah AM, Nazir Y, Naz T, Hassane A, Nosheen S. and Song Y. Evaluation of different standard amino acids to enhance the biomass, lipid, fatty acid, and γ-linolenic acid production in *Rhizomucor pusillus* and *Mucor circinelloides*. Front Nutr. 2022; 9: 876817. http://doi.org/10.3389/fnut.2022.876817

[9] Al Mousa AA, Abo-Dahab NF, Hassane AMA, Gomaa AF, Aljuriss JA. and Dahmash ND. (2022). Harnessing *Mucor* spp. for xylanase production: Statistical optimization in submerged fermentation using agro-industrial wastes. BioMed Res Int. 2022: 3816010. https://doi.org/10.1155/2022/3816010

[10] Al Mousa AA, Abouelela ME, Hassane AMA, Al-Khattaf FS, Hatamleh AA, Alabdulhadi HS, Dahmash ND. and Abo-Dahab NF. Cytotoxic potential of *Alternaria tenuissima* AUMC14342 mycoendophyte extract: A study combined with LC-MS/MS metabolic profiling and molecular docking simulation. Curr Issue Mol Biol. 2022; 44: 5067–5085. https://doi.org/10.3390/cimb44100344

[11] Al Mousa AA, Abouelela ME, Al Ghamidi NS, Abo-Dahab Y, Mohamed H, Abo-Dahab NF. and Hassane AMA. Anti-staphylococcal, anti-*Candida*, and free-radical scavenging potential of soil fungal metabolites: A study supported by phenolic characterization and molecular docking analysis. Curr Issue Mol Biol. 2024; 46: 221–243. https://doi.org/10.3390/cimb46010016

[12] Al Mousa AA, Abouelela ME, Mansour A, Nasr M, Ali YH, Al Ghamidi NS, Abo-Dahab Y, Mohamed H, Abo-Dahab NF. and Hassane AMA. Wound healing, metabolite profiling, and *in silico* studies of *Aspergillus terreus*. Curr Issue Mol Biol. 2024; 46: 11681–11699. https://doi.org/10.3390/cimb 46100694

[13] Abdelrahem MMM, Hassane AMA, Abouelela ME. and Abo-Dahab NF. Comparative bioactivity and metabolites produced by fungal co-culture system against myco-phytopathogens. J Environ Stud. 2023; 31(1): 1–15. https://doi.org/10.21608/jesj.2023.232560.1056

[14] Dreaden EC, Alkilany AM, Huang X, Murphy CJ, El-Sayed MA. The golden age: gold nanoparticles for biomedicine. Chem Soc Rev. 2012; 41(7): 2740–2779. https://doi.org/10.1039/C1CS15237H

[15] Botcha S. and Prattipati SD. Callus extract mediated green synthesis of silver nanoparticles, their characterization and cytotoxicity evaluation against MDA-MB-231 and PC-3 cells. BioNanoSci. 2020; 10: 11–22. https://doi.org/10.1007/s12668-019-00683-3

[16] Kato Y, Suzuki M. Synthesis of metal nanoparticles by microorganisms. Crystals. 2020; 10(7): 589. https://doi.org/10.3390/cryst10070589

[17] Fatima F, Verma SR, Pathak N, Bajpai P. Extracellular mycosynthesis of silver nanoparticles and their microbicidal activity. J Glob Antimicrob Res. 2016; 7: 88–92. https://doi.org/10.1016/j.jgar.2016.07.013

[18] Jaidev LR. and Narasimha G. Fungal mediated biosynthesis of silver nanoparticles, characterization and antimicrobial activity. Colloids Surf B: Biointerface. 2010; 81(2): 430–433. https://doi.org/10.1016/j.colsurfb.2010.07.033

[19] Soni N, Prakash S. Factors affecting the geometry of silver nanoparticles synthesis in *Chrysosporium tropicum* and *Fusarium oxysporum*. Am J Nanotechnol. 2011; 2(1): 112–121. https://doi.org/10.3844/ajnsp.2011.112.121

[20] Yusof HM, Mohamad R, Zaidan UH. and Abdul Rahman N. Microbial synthesis of zinc oxide nanoparticles and their potential application as an antimicrobial agent and a feed supplement in animal industry: a review. J Animal Sci Biotechnol. 2019; 10: 1–22. https://doi.org/10.1186/s40104-019-0368-z

[21] Shkryl YN, Veremeichik GN, Kamenev DG, Gorpenchenko TY, Yugay YA, Mashtalyar DV, Nepomnyaschiy AV, Avramenko TV, Karabtsov AA. and Ivanov VV. Green synthesis of silver nanoparticles using transgenic *Nicotiana tabacum* callus culture expressing silicatein gene from marine sponge *Latrunculia oparinae*. Artif Cells Nanomed Biotechnol. 2018; 46(8): 1646–1658. https://doi.org/10.1080/21691401.2017.1388248

[22] Netala VR, Kotakadi VS, Domdi L, Gaddam SA, Bobbu P, Venkata SK, Ghosh SB. and Tartte V. Biogenic silver nanoparticles: Efficient and effective antifungal agents. Appl Nanosci. 2016; 6: 475–484. https://doi.org/10.1007/s13204-015-0463-1

[23] Fahimirad S, Ajalloueian F. and Ghorbanpour M. Synthesis and therapeutic potential of silver nanomaterials derived from plant extracts. Ecotoxicol Environ Safe. 2019; 168: 260–278. https://doi.org/10.1016/j.ecoenv.2018.10.017

[24] Abdel-Hadi AM, Awad MF, Abo-Dahab NF, Elkady MF. Extracellular synthesis of silver nanoparticles by *Aspergillus terreus*: Biosynthesis, characterization and biological activity. Biosci Biotechnol Res Asia. 2014; 11(3): 1179–1186. https://doi.org/10.13005/bbra/1503

[25] Ottoni CA, Simões MF, Fernandes S, Dos Santos JG, Da Silva ES, de Souza RFB, Maiorano AE. Screening of filamentous fungi for antimicrobial silver nanoparticles synthesis. AMB Express. 2017; 7(1): 1–10. https://doi.org/10.1186/s13568-017-0332-2

[26] Zhao X, Zhou L, Riaz Rajoka MS, Yan L, Jiang C, Shao D, Zhu J, Shi J, Huang Q. and Yang H. Fungal silver nanoparticles: Synthesis, application and challenges. Crit Rev Biotechnol. 2018; 38(6): 817–835. https://doi.org/10.1080/07388551.2017.1414141

[27] Gudikandula K, Vadapally P, Charya MAS. Biogenic synthesis of silver nanoparticles from white rot fungi: Their characterization and antibacterial studies. OpenNano. 2017; 2: 64–78. https://doi.org/10.1016/j.onano.2017.07.002

[28] Hassane AMA, Taha TM, Awad MF, Mohamed H, Melebari M. Radical scavenging potency, HPLC profiling and phylogenetic analysis of endophytic fungi isolated from selected medicinal plants of Saudi Arabia. E-J Biotechnol. 2022; 58: 37–45. https://doi.org/10.1016/j.ejbt.2022.05.001

[29] Lazreg F, Belabid L, Sanchez J, Gallego E, Garrido-Cardenas JA, Elhaitoum A. First report of *Fusarium chlamydosporum* causing damping-off disease on Aleppo pine in Algeria. Plant Dis. 2013; 97(11): 1506. https://doi.org/10.1094/PDIS-02-13-0208-PDN

[30] Mohamed H, Awad MF, Shah AM, Sadaqat B, Nazir Y, Naz T, Yang W, Song Y. Coculturing of *Mucor plumbeus* and Bacillus subtilis bacterium as an efficient fermentation strategy to enhance fungal lipid and gamma-linolenic acid (GLA) production. Sci Rep. 2022; 12(1): 13111. http://doi.org/10.1038/s41598-022-17442-2

[31] Mazrou YS, Makhlouf AH, Elbealy ER, Salem MA, Farid MA, Awad MF, Hassan MM, Ismail M. Molecular characterization of phosphate solubilizing fungi *Aspergillus niger* and its correlation to sustainable agriculture. J Environ Biol. 2020; 41(3): 592–599. http://doi.org/10.22438/jeb/41/3/MRN-1298

[32] Baymiller M, Huang F, Rogelj S. Rapid one-step synthesis of gold nanoparticles using the ubiquitous coenzyme NADH. Matters. 2017. 10081794: 1-4. https://doi.org/10.19185/matters.201705000007

[33] Lotfy WA, Alkersh BM, Sabry SA, Ghozlan HA. Biosynthesis of silver nanoparticles by *Aspergillus terreus*: Characterization, optimization, and biological activities. Front Bioeng Biotechnol. 2021; 9: 633468. https://doi.org/10.3389/fbioe.2021.633468

[34] Mossa MI, Gezaf SA, Ibrahim AA, Hamedo HA. Preliminary screening of endophytic fungi hosted some wild plants in North Sinai for biogenic production of silver nanoparticles. Microb Biosyst. 2023; 8(2): 57–73. https://doi.org/10.21608/mb.2024.341385

[35] Rose GK, Soni R, Rishi P, Soni SK. Optimization of the biological synthesis of silver nanoparticles using *Penicillium oxalicum* GRS-1 and their antimicrobial effects against common food-borne pathogens. Green Process Synth. 2019; 8(1): 144–156. https://doi.org/10.1515/gps-2018-0042

[36] Hashem AH, Saied E, Amin BH, Alotibi FO, Al-Askar AA, Arishi AA, Elkady FM. and Elbahnasawy MA. Antifungal activity of biosynthesized silver nanoparticles (AgNPs) against *Aspergilli* causing aspergillosis: Ultrastructure study. J Funct Biomater. 2022; 13(4): 242. https://doi.org/10.3390/jfb13040242

[37] Saied E, Hussein AS, Al-Askar AA, Elhussieny NI, Hashem AH. Therapeutic effect of biosynthesized silver nanoparticles on hypothyroidism induced in albino rats. E-J Biotechnol. 2023; 65: 14–23. https://doi.org/10.1016/j.ejbt.2023.06.001

[38] Balakumaran MD, Ramachandran R, Balashanmugam P, Mukeshkumar DJ, Kalaichelvan PT. Mycosynthesis of silver and gold nanoparticles: optimization, characterization and antimicrobial activity against human pathogens. Microbiol Res. 2016; 182: 8–20. https://doi.org/10.1016/j.micres.2015.09.009

[39] Nasrollahzadeh M. and Sajadi SM. Green synthesis of Pd nanoparticles mediated by *Euphorbia thymifolia* L. leaf extract: catalytic activity for cyanation of aryl iodides under ligand-free conditions. J Colloid Interface Sci. 2016; 469: 191–195. https://doi.org/10.1016/j.jcis.2016.02.024

[40] Divyalakshmi MV, Thoppil JE. Comparitive study on instrumental characteristics and antibacterial efficacy of green synthesized silver nanoparticles from two pharmacologically important *Garcinia* species: *Garcinia conicarpa* and *Garcinia cambogioides* of Western Ghats. Nanotechnol Environ Eng. 2023; 8(3): 717–732. https://doi.org/10.1007/s41204-023-00320-1

[41] Al-Shmgani HAS, Mohammed WH, Sulaiman GM, Saadoon AH. Biosynthesis of silver nanoparticles from *Catharanthus roseus* leaf extract and assessing their antioxidant, antimicrobial, and wound-healing activities. Artif Cell Nanomed Biotechnol. 2017; 45(6): 1234–1240. https://doi.org/10.1080/21691401.2016.1220950

[42] Naini D, Kumar G, Rawat G, Kapoor S, Kumar R. Process optimization for biogenesis of silver nanoparticles from *Aspergillus flavus* GGRK1 culture filtrate : Characterization and its antibacterial efficacy. Nanofabrication. 2024; 9: 1-16. https://doi.org/10.37819/nanofab.009.1798

[43] Philip D. Biosynthesis of Au, Ag and Au–Ag nanoparticles using edible mushroom extract. Spectrochim Acta A: Mol Biomol Spectrosc. 2009; 73(2): 374–381. https://doi.org/10.1016/j.saa.2009.02.037

[44] Saied E, Abdel-Maksoud MA, Alfuraydi AA, Kiani BH, Bassyouni M, Al-Qabandi OA, Bougafa FHE, Badawy MSEM, Hashem AH. Endophytic *Aspergillus hiratsukae* mediated biosynthesis of silver nanoparticles and their antimicrobial and photocatalytic activities. Front Microbiol. 2024; 15: 1–14. https://doi.org/10.3389/fmicb.2024.1345423

[45] Vijayakumar G, Kim HJ, Jo JW, Rangarajulu SK. Macrofungal mediated biosynthesis of silver nanoparticles and evaluation of its antibacterial and wound-healing efficacy. Int J Mol Sci. 2024; 25(2): 861. https://doi.org/10.3390/ijms25020861

[46] Mohanta YK, Nayak D, Biswas K, Singdevsachan SK, Abd-Allah EF, Hashem A, Alqarawi AA, Yadav D, Mohanta TK. Silver nanoparticles synthesized using wild mushroom show potential antimicrobial activities against food borne pathogens. Molecules. 2018;23(3): 655. https://doi.org/10.3390/molecules23030655

[47] Priyadarshni KC, Krishnamoorthi R, Mumtha C, Mahalingam PU. Biochemical analysis of cultivated mushroom, *Pleurotus florida* and synthesis of silver nanoparticles for enhanced antimicrobial effects on clinically important human pathogens. Inorg Chem Commun. 2022; 142: 109673. https://doi.org/10.1016/j.inoche.2022.109673

[48] Martinez-Gutierrez F, Olive PL, Banuelos A, Orrantia E, Nino N, Sanchez EM, Ruiz F, Bach H, Av-Gay Y. Synthesis, characterization, and evaluation of antimicrobial and cytotoxic effect of silver and titanium nanoparticles. Nanomedicine: Nanotechnol Biol Med. 2010; 6(5): 681–688. https://doi.org/10.1016/j.nano.2010.02.001

[49] Saber SM, Youssef MS, Arafa RF, Hassane AM. Mycotoxins production by *Aspergillus ostianus* Wehmer and using phytochemicals as control agent. J Sci Eng Res. 2016; 3(2): 198–213.

[50] Abdelrahem MMM. Abouelela ME, Abo-Dahab NF, Hassane AMA. *Aspergillus-Penicillium* co-culture: An investigation of bioagents for controlling Fusarium proliferatum-induced basal rot in onion. AIMS Microbiol. 2024; 10(4): 1024–1051. https://doi.org/10.3934/microbiol.2024044

[51] Han JW, Gurunathan S, Jeong J-K, Choi Y-J, Kwon D-N, Park J-K, Kim J-H. Oxidative stress mediated cytotoxicity of biologically synthesized silver nanoparticles in human lung epithelial adenocarcinoma cell line. Nanoscale Res Lett. 2014; 9: 1–14. https://doi.org/10.1186/1556-276X-9-459

[52] Rogers JV, Parkinson CV, Choi YW, Speshock JL, Hussain SM. A preliminary assessment of silver nanoparticle inhibition of monkeypox virus plaque formation. Nanoscale Res Lett. 2008; 3: 129–133. https://doi.org/10.1007/s11671-008-9128-2

[53] Morones JR, Elechiguerra JL, Camacho A, Holt K, Kouri JB, Ramírez JT, Yacaman MJ. The bactericidal effect of silver nanoparticles. Nanotechnology. 2025; 16(10): 2346. https://doi.org/10.1088/0957-4484/16/10/059

[54] Gharpure S, Yadwade R, Ankamwar B. Non-antimicrobial and non-anticancer properties of ZnO nanoparticles biosynthesized using different plant parts of *Bixa orellana*. ACS Omega. 2022; 7(2): 1914-1933. https://doi.org/10.1021/acsomega.1c05324

[55] Andleeb A, Andleeb A, Asghar S, Zaman G, Tariq M, Mehmood A, Nadeem M, Hano C, Lorenzo JM, Abbasi BH. A systematic review of biosynthesized metallic nanoparticles as a promising anti-cancer-strategy. Cancers. 2021; 13: 2818. https://doi.org/10.3390/ cancers13112818

[56] Cao D, Shu X, Zhu D, Liang S, Hasan M, Gong S. Lipid coated ZnO nanoparticles synthesis, characterization and cytotoxicity studies in cancer cell. Nano Converg. 2020; 7: 14. https://doi.org/10.1186/s40580-020-00224-9

[57] Moubasher AH, El-Naghy MA, Abdel-Hafez SII. Studies on the fungus flora of three grains in Egypt. Mycopathol Mycol Appl. 1972; 47: 261–274. https://doi.org/10.1007/BF02051664

[58] Mohamed H, El-Shanawany A, Shah AM, Nazir Y, Naz T, Ullah S, Mustafa K, Song Y. Comparative analysis of different isolated oleaginous Mucoromycota fungi for their γ-linolenic acid and carotenoid production. BioMed Res Int. 2020: 3621543. https://doi.org/10.1155/2020/3621543

[59] Devi L, Joshi S. Ultrastructures of silver nanoparticles biosynthesized using endophytic fungi. J Microsc Ultrastr. 2015; 3(1): 29. https://doi.org/10.1016/j.jmau.2014.10.004

[60] Yassin MA, Elgorban AM, El-Samawaty AE-RMA, Almunqedhi BMA. Biosynthesis of silver nanoparticles using *Penicillium verrucosum* and analysis of their antifungal activity. Saudi J Biol Sci. 2021; 28(4): 2123–2127. https://doi.org/10.1016/j.sjbs.2021.01.063

[61] Khalaf NH, Hassane AMA, El-Deeb BA, Abo-Dahab NF. Antimicrobial efficacy mediated by mycogenic and characterized selenium nanoparticles. Sohag J Sci. 2024; 9(3): 255-260. https://doi.org/10.21608/sjsci.2024.254285.1161

[62] Al Mousa AA, Mohamed H, Hassane AMA, Abo-Dahab NF. Antimicrobial and cytotoxic potential of an endophytic fungus *Alternaria tenuissima* AUMC14342 isolated from *Artemisia judaica* L. growing in Saudi Arabia. J King Saud Univ-Sci. 2021; 33: 101462. https://doi.org/10.1016/j.jksus.2021.101462

[63] Mohamed H, Hassane A, Rawway M, El-Sayed M, Gomaa A, Abdul-Raouf U, Shah AM, Abdelmotaal H, Song Y. Antibacterial and cytotoxic potency of thermophilic *Streptomyces werraensis* MI-S.24-3 isolated from an Egyptian extreme environment. Arch Microbiol. 2021; 203: 4961–4972. https://doi.org/10.1007/s00203-021-02487-0

[64] Jahangirian H, Haron MDJ, Shah MH, Abdollahi Y, Rezayi M, Vafaei N. Well diffusion method for evaluation of antibacterial activity of copper phenyl fatty hydroxamate synthesized from canola and palm kernel oils. Digest J Nanomater Biostuctr. 2013; 8(3): 1263–1270.

[65] Gebreyohannes G, Nyerere A, Bii C, Sbhatu DB. Determination of antimicrobial activity of extracts of indigenous wild mushrooms against pathogenic organisms. Evid-Based Complement Altern Med, 2019; 2019: 6212673. https://doi.org/10.1155/2019/6212673

[66] Moshi MJ, Van den Beukel C, Hamza OJ, Mbwambo ZH, Nondo RO, Masimba PJ, Matee M, Kapingu MC, Mikx F, Verweije P. Brine shrimp toxicity evaluation of some Tanzanian plants used traditionally for the treatment of fungal infections. Afr J Tradit Complement Altern Med. 2007; 4(2): 219-225. https://doi.org/10.4314/ajtcam.v4i2.31211

[67] Skehan P, Storeng R, Scudiero D, Monks A, McMahon J, Vistica D, Warren JT, Bokesch H, Kenney S, Boyd MR. New colorimetric cytotoxicity assay for anticancer-drug screening. J Nat Cancer Inst. 1990; 82(13): 1107-1112. https://doi.org/10.1093/jnci/82.13.1107

[68] Alsehli BR, Hassan MHA, Mohamed DS, Saddik MS, Al-Hakkani MF. Enhanced cytotoxic efficacy against MCF-7 and HCT116 cell lines and high-performance cefoperazone removal using biogenically synthesized CeO_2 nanoparticles. J Mol Struct. 2024; 1318: 139261. https://doi.org/10.1016/j.molstruc.2024.139261